Pergamon

Cement and Concrete Research, Vol. 26, No. 6, pp. 919-931, 1996

0008-8846/96 $15.00 + .00

PII S0008-8846(96)00066-X

# FROST DURABILITY OF HIGH STRENGTH CONCRETE: EFFECT OF INTERNAL CRACKING ON ICE FORMATION

**Stefan Jacobsen[1], Erik J. Sellevold[2] and Seppo Matala[3]**
[1]The Norwegian Building Research Institute, Oslo, Norway,
[2]The Norwegian Institute of Technology, Trondheim, Norway,
[3]Helsinki University of Technology, Finland

(Refereed)
(Received September 11, 1995; in final form March 29, 1996)

## ABSTRACT

Ice formation measurements using low temperature calorimetry (CAL) were made on non-air entrained high strength concretes (HSC) before and after exposure to rapid freeze/thaw cycles in water (ASTM C666 proc. A). The purpose was to explore the relationship between water absorption during test, changes in ice formation and deterioration, to investigate the deterioration mechanism of non-air entrained HSC in the ASTM C666 test. CAL results showed zero or very little ice formation in the concretes (w/b = 0.40 and 0.35, 0, 5 and 8 % silica fume) before C666 testing in the temperature range of the test (-20 °C). After the test (DF = 10 - 11) significant water absorption had taken place. Only one half or less of the absorbed water was freezeable to - 20 °C, i.e. only part of the absorbed water goes into the created cracks and contributes to the deterioration by freezing there. The rest of the water is freezeable at lower temperatures or so tightly bound that it does not freeze at all to -55 °C. The freezeable water to -20 °C after test constitutes 3 - 7 vol-% of the cement paste. CAL measurements at intermediate stages of deterioration show very rapid transitions between no and significant amount of freezeable water, and indicate a progressive mechanism of deterioration, starting at the surface in contact with water and moving inward. Apparently very little ice formation can initiate the process and result in major damage. Water storage after freeze/thaw testing results in self healing characterized by significant recovery of dynamic E-modulus and decreased amounts of ice formation. However, compressive strength recovery is much smaller than the recovery of E-modulus.

## Introduction and Scope

In a previous investigation (1), two low temperature calorimetry (CAL) tests of ice formation were performed on a non-air entrained high strength concrete with w/c + s = 0.30 and 8 % silica

fume before freeze/thaw exposure in ASTM C666 procedure A, and after 300 cycles with some internal cracking (Durability Factor = 79). The results of the CAL measurements (specimens sawn from the concrete beams and tested in the actual moisture condition of the beam) showed almost zero increase in freezeable water down to -8 °C; from 3.3 to 3.5 % of evaporable water content. A more significant increase in total amount of freezeable water down to - 55 °C was observed; from 10.8 % to 16.4 %. The evaporable water content in large slices sawn next to the calorimeter specimens increased much more than the ice formation. It was difficult to believe that the very small increase in freezeable water in the temperature range of the freeze/thaw test could have initiated damage. Further, most of the absorbed water was not freezeable in the temperature range of the freeze/thaw test.

In earlier investigations by Verbeck and Klieger, (2), freezeable water was measured in lower quality concretes before and after freeze/thaw exposure. They measured significant increases in freezeable water content in the temperature range of the frost test (-20 °C) in concrete specimens of w/c = 0.49 - 0.72 that had been damaged by freeze/thaw.

In the present paper some further investigations of the increase in amount of freezeable water measured by CAL during the course of deterioration by the ASTM C666 procedure A test have been performed on concretes with water/binder ratio 0.35 and 0.40. The purpose of the investigation was to study the relationship between freezeable water and internal cracking and, if possible, to follow the progress of damage as measured by increase in freezeable water content and changes in pore structure. In addition, the self healing of frost deteriorated beams has been investigated.

Low temperature calorimetry is a very useful tool in the investigation of pore structure in hardened portland cement products, due to the ability of testing specimens without preparation involving drying that may alter the pore structure. Sellevold, Bager et al (3, 4, 5, 6, 7 and more) have described the use of low temperature calorimetry closer: calculation of freezeable water in different temperature intervals, the method of assessing pore structure properties by the use of freezing point depression and investigations of pore structure properties of various cement pastes. When testing high strength concrete in low temperature calorimetry, the amount of paste in the specimen is relatively small and may vary between parallel specimens. In addition the freezeable water content is low, (8). In this paper the tests have therefore been performed using 2 or 3 parallel specimens for each variable studied.

## Experimental

In table 1 the main properties of the concretes investigated are given. The concretes are part of an investigation of frost testing of concrete involving also other investigations (9-13). The concrete specimens were 100 by 100 by 500 mm beams, water stored after demoulding (24 h) and up to testing (3 months for 040-00 and 040-05 and 28 days for 035-08). Before freeze/thaw

TABLE 1
Concretes Tested in ASTM C666 Procedure A, and by CAL

| Mix | w/(c+s) | s/(c+s) | Cement (kg/m$^3$) | Aggregate 3) (kg/m$^3$) | Slump (cm) | Air (vol-%) (fresh) | Air (vol-%) (hardened) | $f_c$ 28 (MPa) |
|---|---|---|---|---|---|---|---|---|
| 040-00 | 0.40 | 0 | 432 1) | 1799 | 20 | 1.6 | 2.0 | 69 |
| 040-05 | 0.40 | 0.05 | 409 1) | 1782 | 19 | 2.0 | 2.3 | 79 |
| 035-08 | 0.35 | 0.08 | 440 2) | 1765 | 21 | 1.4 | 1.8 | 105 |

1), 2) Norwegian OP and High Strength cement, 3) $D_{max}$ 16 mm (Årdal Norway, granite).

testing the beams were sawn to 345 mm lengths to fit into the boxes for freeze/thaw in water. The rest of the beams were used for various purposes, among others CAL (Ø = 15, h = 70 mm sawn cylinders) and moisture condition determination (slices 100 by 100 by 20-30 mm) at start of freeze/thaw testing.

Measurements of evaporable water contents ($w_e$) before frost exposure (virgin condition) were performed by weighing and drying slices at 105 °C. Subsequently suction porosities of the slices were measured by immersion in water, and macro porosity was measured by the amount of water forced in at 10 MPa pressure (14). These measurements showed that the suction porosity ("gel + capillary" pores) were filled before the frost test within the accuracy of this simple test. Measurements of absorption during water curing indicated that self-desiccation pores were filled during curing. Table 2 shows the results of ASTM C666 testing: relative dynamic moduli and Durability Factor (DF). Specimens for CAL were taken from the beams after frost exposure at the relative dynamic moduli given in table 2. It is important to note that the self-healing (measured after 3 months storage in water of 20 °C after stop ASTM test) only gave minor recovery of the strength, in spite of the large recovery of resonance frequency (11).

Specimens for testing in the calorimeter were taken before test and at the intervals given in table 2. The slices were taken from the centre (middle) of the beams. First slices of 15 mm thickness were wet sawn perpendicular to the length axis of the beam. Then calorimeter specimens were wet sawn with a fine diamond saw into cylinders with diameter 14 - 15 mm and height 70 mm to fit into the calorimeter cell. The calorimeter specimens were taken perpendicular to the top (trowelled) surface of the beams, excluding the 15 mm at top and bottom. Immediately after sawing, the samples were weighed and isolated in small tight plastic bags stored in small tight bottles. The weight of the specimens were checked again before calorimeter test. Negligible changes in weights were registered. Calorimeter tests were performed 1 - 3 weeks after stop of freeze/thaw for the 040-00 and 040-05 concretes and after maximum 1 week for the 035-08 concrete. Also larger slices (100 by 100 by 20 - 30 mm) were sawn from the beams, next to the calorimeter specimens, for more accurate determination of moisture content. It is anticipated that the influence of wet sawing will be much smaller on the larger slices than on the small calorimeter specimens. To investigate variations in freezeable water content due to variations in paste content, three parallel calorimeter specimens were tested before and after frost deterioration for the 040-00 and 040-05 concretes. Two parallel specimens were tested for the 035-08 concrete and one specimen after self healing for each of the 040-00 and 040-05 concretes. At 49 cycles of the 035-08 concrete, one specimen was taken from the middle of the beam (normal procedure) and one specimen was taken close to the end surface of the beam in the same manner as for the other specimens.

TABLE 2
Results of Freeze/Thaw Testing

| Mix | Relative dynamic modulus ($E_{stop}/E_{start}$) | | | | | DF 1) |
|---|---|---|---|---|---|---|
| | 0 cy | 35 cy | 49 cy | 69/70 cy | Healing | |
| 040-00 | 1.00 | - | - | $0.51_{70}$ | 0.98 | 11 |
| 040-05 | 1.00 | - | - | $0.23_{70}$ | 0.72 | 10 |
| 035-08 | 1.00 | 0.94 | 0.78 | $0.31_{69}$ | - | 11 |

1) Durability Factor: $(E_{300}/E_{start}) \geq 0.60$, then $DF = (E_{300}/E_{start})$
$(E_{300}/E_{start}) < 0.60$, then $DF = 0.60 \cdot (N_{E_{rel}=0.6}/300)$

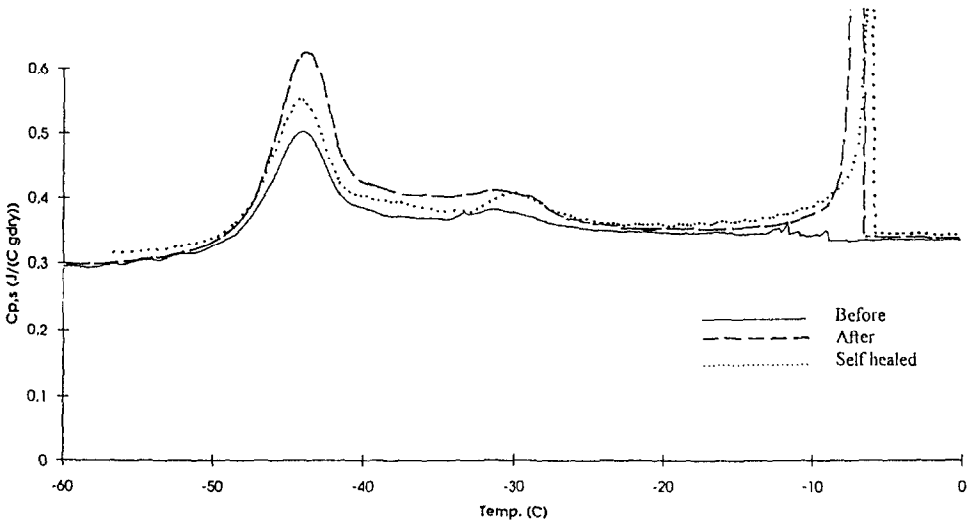


FIG. 1.
Heat flow vs. calorimeter block temperature during cooling for concrete 040-00.

The calorimeter used was a Calvet BT 2.15 D micro calorimeter at Helsinki University of Technology in Finland. The specimens were cooled to -60 °C at 3.0 °C/h and heated at 4.2 °C/h. Before testing, the specimens were weighed and sprinkled with a few milligrams of AgI to reduce super cooling as suggested by Fontenay and Sellevold (4). Aluminium oxide was used in the reference cell. Heat flow (dq/dt), time interval (dt) and calorimeter block temperature (T) were logged every 30 seconds and stored in personal computer worksheets for further calculations. The heat flow dq/dt [W = J/s] given in the output data included the sensitivity of the calorimeter. Apparent heat capacity, $C_{pa,s}$ [J/(°C $g_{dry}$)] was calculated as function of temperature:

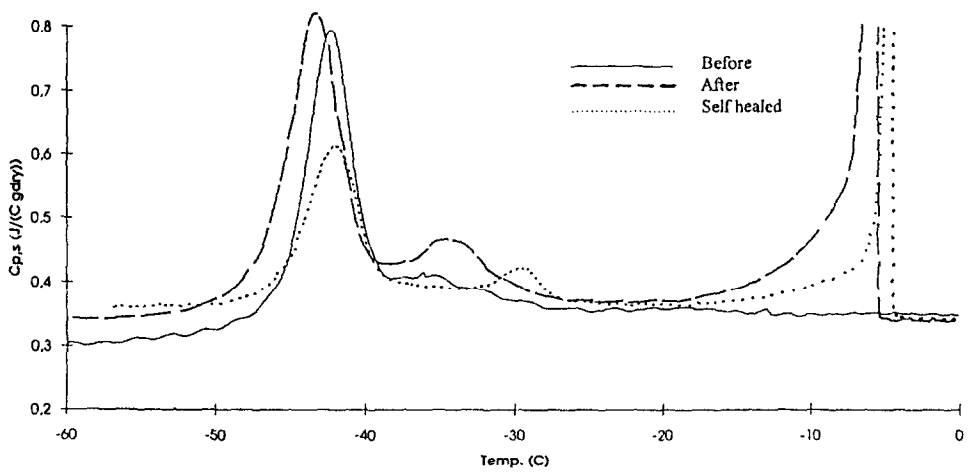


FIG. 2.
Heat flow vs. calorimeter block temperature during cooling for concrete 040-05.

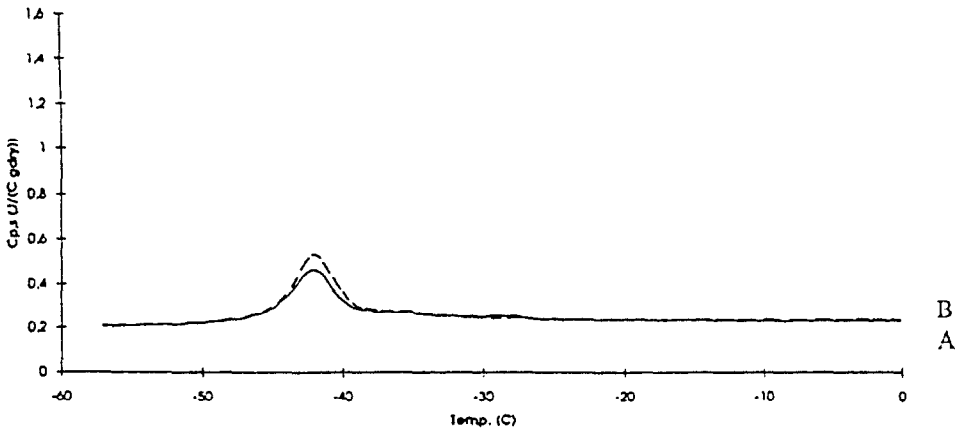


FIG. 3.
Heat flow vs. block temperature during cooling, concrete 035-08 after 35 cycles (two samples).

$$C_{pa,s} = \frac{\frac{dq}{dt}[J/s]}{\frac{dT}{dt}[°C/s] \cdot m[g]} \quad (1)$$

In figures 1 - 7 apparent heat capacities are plotted versus calorimeter block temperature. Integrated heat down to a temperature T ($q_T$ [$J/g_{dry}$]) was calculated by integrating the product of measured heat flow and time interval (dt) at each logging:

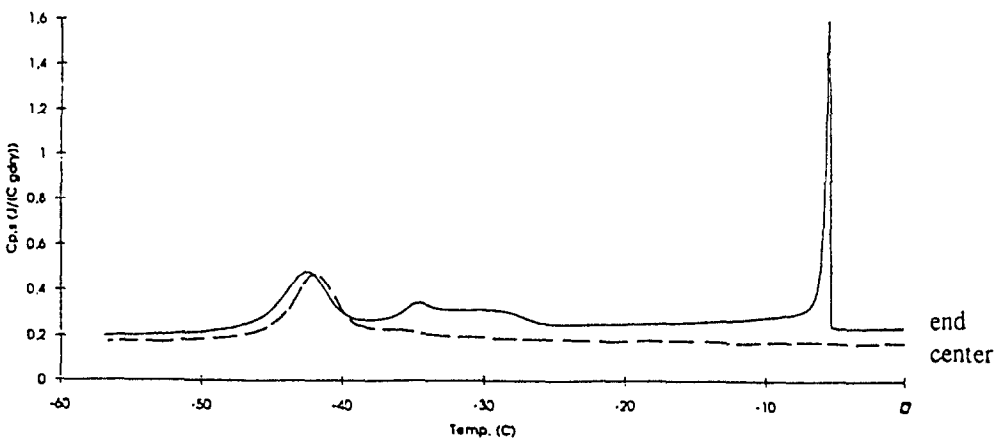


FIG. 4.
Heat flow vs. calorimeter block temperature during cooling for concrete 035-08 after 49 cycles (two samples: one from centre and one from end of beam).

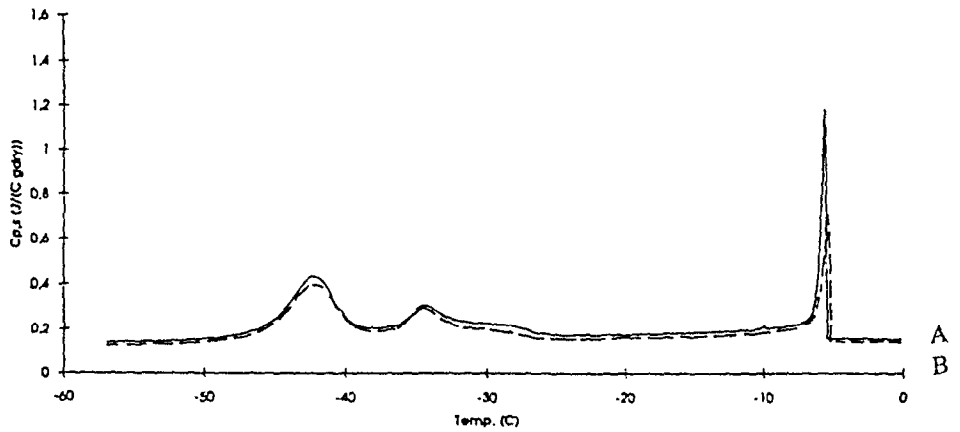


FIG. 5.
Heat flow vs. calorimeter block temperature (cool) concrete 035-08 after 69 cycles (two samples).

$$q_T = \int C_{pa,s} dT = \frac{1}{m} \int \frac{dq}{dt} \cdot dt \tag{2}$$

Amount of ice formed in different temperature intervals: $w_f$ [mg/$g_{dry}$] (dried at 105 °C to constant weight) was then calculated according to the principles described by Fontenay and Sellevold (4) ("DTH-BML method").

amount of ice $$w_f = (q_T'/\Delta h_f) \quad [g/g_{dry}] \tag{3}$$

heat of fusion of water, (3): $$\Delta h_f = 333.6 + 2.22 \cdot T(°C) \quad [J/g] \tag{4}$$

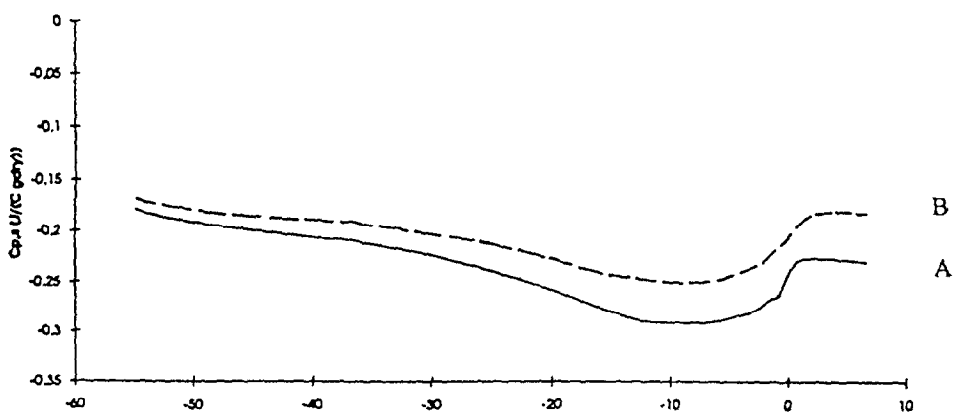


FIG. 6.
Heat flow vs. calorimeter block temperature (heat) concrete 035-08 at 0 cycles (two samples).

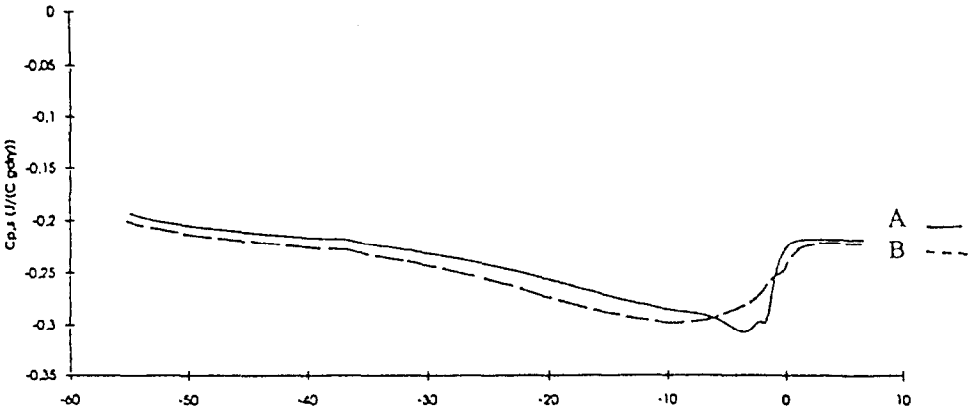


FIG. 7.
Heat flow vs. calorimeter block temperature (heat) concrete 035-08 after 35 cycles (two samples).

The amount of ice formed in a temperature interval is approximately proportional to the area under the heat flow curve with a linear baseline extension from first freezing to - 55 °C. A corrected $q_T'$ must be calculated. To do this some assumptions are made for the construction of the corrected baseline. This correction takes into account the change in heat capacity of the specimen due to phase transitions during the calorimeter test, since a portion of the change in $C_{pa,s}$ is due to the difference in heat capacity between water and ice. Heat capacity of water, $C_{p,\ H2O}$ is 4.184, and heat capacity of ice, $C_{p,\ ice}$ is 2.092 [J/(°C · g)]. In table 3 "increment" denotes

TABLE 3
Ice Formation ($w_f$) to Different Temperatures and Evaporable Water ($w_e$) as $mg/g_{dry}$

| Concrete | E-rel | $w_f$ cool | | | | | $w_f$ heat | | | | $w_e$ | $w_f$ -55 | $w_{nf}$ -55 |
|---|---|---|---|---|---|---|---|---|---|---|---|---|---|
| | | Total | Increment (accumulated) | | | | Total | Increment (accum.) | | | CAL | cool | cool |
| | | -55 | -10 | -20 | -55 | Δ (-10-55) | -55 | -10 | -55 | Δ (-10-55) | spec. | / $w_e$ % | |
| 040-00: | | | | | | | | | | | | | |
| Before, B | 1.00 | 9 | 0 | 1 | 10 | 10 | 10 | 4 | 10 | 7 | 46 | 20 | 37 |
| After, A | 0.51 | 16 | 4 | 5 | 16 | 12 | 17 | 9 | 17 | 8 | 53 | 30 | 38 |
| Healed, H | 0.98 | 11 | 2 | 3 | 12 | 10 | 12 | 6 | 12 | 6 | 51 | 22 | 40 |
| Δ(A-B) | | 7 | 4 | 4 | 7 | | 7 | 5 | 7 | | 8 1) | | |
| Δ(H-B) | | 2 | 2 | 2 | 2 | | 2 | 2 | 2 | | 1 | | |
| 040-05: | | | | | | | | | | | | | |
| Before, B | 1.00 | 11 | 0 | 1 | 11 | 11 | 12 | 4 | 12 | 8 | 48 | 23 | 37 |
| After, A | 0.23 | 22 | 6 | 8 | 22 | 17 | 23 | 13 | 23 | 11 | 64 | 34 | 42 |
| Healed, H | 0.72 | 12 | 4 | 5 | 12 | 9 | 12 | 7 | 12 | 5 | 64 | 18 | 52 |
| Δ(A-B) | | 11 | 6 | 7 | 11 | | 11 | 9 | 11 | | 16 | | |
| Δ(H-B) | | 1 | 4 | 4 | 1 | | 1 | 3 | 1 | | 16 | | |
| 035-08: | | | | | | | | | | | | | |
| 0 cy | 1.00 | 7 | 0 | 0 | 7 | 7 | 6 | 1 | 6 | 4 | 45 | 16 | 38 |
| 35 cy | 0.94 | 7 | 0 | 0 | 7 | 7 | 7 | 2 | 8 | 5 | 49 | 14 | 42 |
| 49 cy mid | 0.78 | 7 | 0 | 0 | 7 | 7 | 7 | 2 | 7 | 5 | 46 | 14 | 40 |
| 49 cy end | 0.78 | 14 | 3 | 4 | 14 | 11 | 14 | 9 | 15 | 6 | 56 | 24 | 43 |
| 69 cy | 0.31 | 13 | 2 | 3 | 13 | 11 | 13 | 7 | 13 | 6 | 54 | 23 | 41 |

1) Rounded off

that ice formation was calculated in several temperature intervals, and presented as accumulated ice formation down to -10, -20 and -55 °C, using equation (4). In this case baseline corrections for change in heat of fusion, and amount of ice $w_f = (q_T'/\Delta h_f)$, were calculated in each temperature interval. "Total" is calculated using a somewhat different approach, Fontenay and Sellevold (4), and serves as a control of the increment method. "Cool" denotes that calculations are made from solidification thermograms. "Heat" denotes that calculations are made from melting thermograms. Further details and assumptions are given by Fontenay and Sellevold (4), and by Bager (7).

## Results

In table 3 ice formation ($w_f$) down to different temperatures are given for the concretes before frost deterioration, at various degrees of deterioration and after self healing. Also evaporable water ($w_{e\ cal\ spec}$), and non-freezeable water contents ($w_{nf\text{-}55}$) in the specimens are given.

Figures 1 and 2 show heat flow vs. calorimeter block temperature (cool) for the 040-00 and 040-05 concretes before and after frost deterioration and after self healing. Figures 3 - 7 show heat flow vs. calorimeter block temperature for the 035-08 concrete at various levels of deterioration. Table 4 gives evaporable water contents for the small calorimeter samples and the large slices. Table 5 gives the variation in freezeable water between three parallel samples after frost deterioration for concretes 040-00 and 040-05, expressed as $g/g_{dry}$ and as % of evaporable water.

## Discussion

General. Table 3 gives calculated amounts of ice. Table 4 gives the evaporable water contents of the small calorimeter specimens and the larger slices cut next to the calorimeter specimens. We see that there is no clear tendency towards higher water content in the small

TABLE 4
Evaporable Water Content in Small CAL Specimens and Large Concrete Slices

| Mix | E rel | $w_e$ ($g/g_{dry}$) | |
|---|---|---|---|
| | | CAL spec. | Large slices |
| 040-00: | | | |
| Before, B | 1.00 | .0458 | .0497 |
| After, A | 0.51 | .0533 | .0541 |
| Healed, H | 0.98 | .0510 | .0540 |
| 040-05: | | | |
| Before, B | 1.00 | .0479 | .0500 |
| After, A | 0.23 | .0643 | .0584 |
| Healed, H | 0.72 | .0635 | .0541 |
| 035-08: | | | |
| 0 cy | 1.00 | .0449 | .0487 |
| 35 cy | 0.94 | .0487 | .0492 |
| 49 cy mid | 0.78 | .0464 | .0494 |
| 49 cy end | 0.78 | .0562 | .0506 |
| 69 cy | 0.31 | .0537 | .0580 |

calorimeter samples than in the large slices due to the wet-sawing, but random variation as expected from varying aggregate/paste ratio. Table 5 gives the variation in freezeable water between 3 parallel calorimeter samples. The coefficient of variation is maximum 11 % expressed as $g/g_{dry}$ and maximum 6 % when expressed as percentage of $w_e$. The main uncertainty with small specimens therefore appears to be the uneven distribution of aggregate and paste in the samples.

From table 3 we see that amounts of ice calculated from heat curves ($w_{f\text{-}10}$) are markedly larger than $w_{f\text{-}10}$ from cooling curves, i.e. ice in the pores melts at a higher temperature than it forms. According to Sellevold and Bager (3) a major reason for this hysteresis is bottleneck effects, i.e. that melting is controlled by the cavity of the pore, whereas freezing is controlled by a moving ice front into narrow pore openings. Similar hysteresis is observed in adsorption/ desorption experiments and mercury intrusion/extrusion cycles. Matala (15) has recently reviewed various causes for hysteresis between freezing and melting.

From table 3 we also see that "increment" and "total" amounts of ice ($w_{f\text{-}55}$) calculated from both heat and cool are in good agreement.

From table 3 and 4 we see how evaporable water content ($w_e$) increases with increasing number of cycles. This increased absorption during freeze/thaw has been discussed previously (11,13). We also see that the increase in evaporable water on freeze/thaw deterioration is larger than the increase in freezeable water, in agreement with earlier observations (1). This will be discussed in more detail below.

Ice Formation 040-00 and 040-05 - Cracking and Healing. Both the calculated amount of ice (table 3) and the calorimeter curves before frost exposure (figures 1 and 2) show practically no ice formation down to - 10 °C, and 1 $mg/g_{dry}$ down to - 20 °C on cooling. From table 3 we see

TABLE 5
Variation in Total Freezeable Water ($w_{f\text{-}55}$), Cooling

| Specimen - Mix | $w_{f\text{-}55}$ ($g/g_{dry}$) | $w_{f\text{-}55}$ (% of $w_e$) |
|---|---|---|
| 1 | .0084 | 20.5 |
| 2 | .0100 | 20.2 |
| 3 | .0095 | 20.1 |
| mean 040-00 before | .0093 | 20.3 |
| coeff. of var. (%) | 9 | 1 |
| 1 | .0139 | 29.4 |
| 2 | .0173 | 29.8 |
| 3 | .0163 | 29.9 |
| mean 040-00 after | .0158 | 29.7 |
| coeff. of var. (%) | 11 | 1 |
| 1 | .0115 | 23.1 |
| 2 | .0099 | 22.4 |
| 3 | .0111 | 22.3 |
| mean 040-05 before | .0108 | 22.6 |
| coeff. of var. (%) | 8 | 2 |
| 1 | .0218 | 33.3 |
| 2 | .0224 | 36.7 |
| 3 | .0220 | 33.2 |
| mean 040-05 after | .0221 | 34.4 |
| coeff. of var. (%) | 1 | 6 |

that the increase in amount of freezeable water from 0 to -10 °C (primary freezing) after frost deterioration is 4 - 6 $mg/g_{dry}$ (cool), whereas the evaporable water increased 8 - 16 $mg/g_{dry}$. The increased primary ice formation can be seen as a large peak on the "After" curves in figure 1 and 2. The increase down to -20 °C (cool) due to frost deterioration is 4 and 7 $mg/g_{dry}$. The increase in total freezeable water (cool -55 °C) for 040-00 and 040-05 is 7 and 11 $mg/g_{dry}$ after deterioration. A large part of the increase in freezeable water due to frost deterioration therefore takes place in the primary part of the calorimeter curve just below zero (see figures 1 and 2), i.e. water close to bulk state in large pores or cracks. The silica fume concrete 040-05 has the largest increase in freezeable water on deterioration. This is also the concrete that was deteriorated most and increased its evaporable water content most. From the increment values we also see that there are increases in amount of water that is freezeable only in the low temperature region from -20 - -55 °C (on cool) and -10 - -55 °C (on heat) due to frost deterioration. As already pointed out, the increase in evaporable water is the same as the increase in total ice for 040-00, while for 040-05 the evaporable water is 50 % higher than the ice increase. The results are in line with the observations in (1): that there is a significant increase in water content that is freezeable only in the low temperature region after freeze/thaw or not freezeable at all, i.e. water uptake does not take place only in large pores and cracks.

After self healing we see from table 3 that the amount of freezeable water is reduced significantly, both in primary freezing and in the low temperature region. From figures 1 and 2 we see for the self healed concretes (dotted lines) that the primary peaks are narrower compared to the peaks right after deterioration, illustrating the reduced primary ice formation and reduced amount of coarse (continuous) pores after self-healing. However, there is still a significant amount of freezeable water in the primary region, showing that a permanent increase in the coarse porosity has taken place. From table 4 we see that $w_e$ is reduced or unchanged after healing. From the low temperature region of figures 1 and 2 we see that the transition around -40 °C that was increased in strength by frost deterioration is also reduced. For the 040-05 concrete this peak is even reduced below the initial (undamaged) state. Further, a new transition is occurring around -30 °C after healing. This shift towards intermediate freezing temperatures between the primary and the low temperature transition, indicates a pore refinement at the reduction of the primary peak, or a coarsening of fine pores at the reduction of the peak around - 40 °C, in accordance with the observations of rehydration products and reduced porosity after self healing (10,12).

Further, table 3 and figure 1 and 2 show that 040-05 (silica fume) has more freezeable water in the low temperature region than 040-00 (OPC), in accordance with (16). Further, $w_{f\text{-}55}$ is a rather small portion of $w_e$: 20 - 34 %. This is in good agreement with (4, 5), where $w_{f\text{-}55}/w_e$ = 0.21 - 0.57, when w/c = 0.40 - 0.70.

Ice Formation 035-08 - Damage Progression. For the 035-08 concrete the calorimeter specimens were taken from concrete beams with varying degrees of deterioration. As already noted (table 4) evaporable water content increased with number of cycles. From table 3 we see that the primary freezing is negligible after 0, 35 and 49 cycles for specimens taken at the centre of the beams. The relative dynamic moduli for these beams were 1.00, 0.94 and 0.78 respectively. For the two specimens at 69 cycles and one specimen from the end of the beam after 49 cycles we see that there are large increases in amount of freezeable water in the primary region in the same way as noted for the 040-00 and 040-05 concretes. The results after 49 cycles show that the internal cracking before total breakdown can be very unevenly distributed within one specimen. By visual observation of the beams, very few thin cracks could be seen (unevenly spread out) on the surface. The results of ice formation measurements indicate a rather rapid transition from zero to large primary ice formation in the concrete on rapid freeze/thaw in water,

and a progression from the surface (end) and inward (centre). The differences in ice formation and cracking between end and centre of beam also correlated with increases in evaporable water content both in the small calorimeter specimens and in larger slices cut from the end and centre of the beam. From the amount of ice calculated from the heat curves (table 3) we see that there are some small differences between the specimen at 0 cycles and the specimens at 35 and 49 cycles, even though none of these specimens showed primary freezing on cooling. The amount of ice formed (heat) is a little higher for the specimens that have undergone 35 and 49 freeze/thaw cycles, possibly as an early stage of deterioration. The ratios $w_{f\text{-}55}/w_e$ are lower than for the 0.40 concretes, showing that an even smaller part of the evaporable water is freezeable in this higher strength concrete.

Figures 3, 4 and 5 show the progression in increased ice formation on cool. In each of the figures the two parallel specimens are plotted. From the deteriorated concretes with clear primary peaks in figure 4 and 5 (49 and 69 cycles) we see that the transitions arising around -30 - -35 °C for these concretes with higher strength are more pronounced than for the 040-concretes after deterioration (figures 1 and 2). Figures 6 and 7 show heat flow during heating of 035-08 at 0 and 35 cycles. We can see that one of the samples after 35 cycles has a sudden melting around zero, whereas the samples with 0 cycles and the other sample with 35 cycles show a more gradual melting. None of these specimens have any primary ice formation on cooling. The results may indicate (as discussed above) an early stage of deterioration where some changes have occurred in the pore structure due to the freeze thaw exposure.

Non-freezeable water (non-freezeable at - 55 °C, $w_{nf} = w_e - w_f$), increases for all concretes at frost deterioration (and self healing), compared to Before, see last column of table 3.

Relation Ice Formation - Frost Durability. Earlier experiences (1, 8) showed that high strength concretes with very low primary ice formation had rather bad performance in the ASTM C666 procedure A freeze/thaw test. The results (1) showed that for a high strength concrete with Durability Factor = 79, the deterioration by rapid freeze/thaw in water and the accompanying water uptake was not reflected in increased primary ice formation. This was quite surprising. The present concretes were deteriorated much more (Durability Factors = 10 - 11), and the ice formation measurements clearly showed that this deterioration led to a large primary ice formation. However, only a part of the water absorbed on freeze/thaw is freezeable. From table 3 we see that a large part of the absorbed water is bound very strongly so that it cannot freeze even at -55 °C. The freezeable part is smallest for the concrete with highest strength (035-08). In that case only about 25 % of the increase in evaporable water due to frost deterioration could be measured as increase in freezeable water down to -10 °C (cool). Before deterioration zero primary freezing was measured. Therefore rather small increase in freezeable water content is associated with large damage. Fagerlund (17) claimed that freezeable water content smaller than 1 % of cement paste volume is sufficient to damage HSC if the water is freezing in "closed container" pores. In the present concretes 0.001 $g/g_{dry}$ water is approximately 1 vol-% of the paste fraction. The water absorbed on deterioration is 3 - 7 vol-% of paste, see $\Delta$(A-B) in table 3.

The accelerated absorption on freeze/thaw makes ice formation measurements on virgin, non-freeze/thaw tested specimens unable to predict the performance of concrete in freeze/thaw tests in water, i.e. no primary ice formation in the test range does not necessarily imply no frost damage. The measurements in (13) show that water absorption during freeze/thaw can take place even in concretes with no signs of internal cracking during the 300 cycles of the ASTM C666 test, and practically no scaling in salt/frost scaling tests.

High primary ice formation was observed in one specimen taken close to the end of the beam, whereas no primary ice was observed in a specimen taken from the centre of the same

TABLE 6
Pores with Radius < 55 Å by CAL (-10 °C) and MIP (Reference (12)) (vol-% of Concrete)

| Specimen | CAL | | MIP |
|---|---|---|---|
| | Heat | Cool | |
| 040-00: | | | |
| Before | 0.9 | 0 | 1.1 |
| After | 2.0 | 0.9 | 1.4 |
| Healed | 1.3 | 0.4 | 1.0 |
| 040-05: | | | |
| Before | 0.9 | 0 | 1.5 |
| After | 2.9 | 1.3 | 2.1 |
| Healed | 1.6 | 0.8 | 1.2 |

beam at the same stage of deterioration. Therefore we expect the absorption and ice formation to be largest close to the surface. This indicates that the deterioration in the present freeze/thaw test is progressive, starting at the surface (end) where the absorption increases the water content first.

Relation Ice Formation - Mercury Intrusion. Table 6 shows amount of pores with radius smaller than 55 Å (i.e. pore water frozen below -10 °C) calculated according to Sellevold and Bager (3), and as measured by Mercury Intrusion Porosimetry (MIP) (12). From the table we see that the MIP - values are close to or between the values calculated from heating and cooling in the calorimeter. This is in accordance with the results (3). As already noted, it was argued (3) that the ice progresses as a front trough the material during freezing. It is therefore most correct to compare the ice formation on cooling with the MIP-results. Drying of MIP-specimens before testing is known to alter the pore structure (5), and is a major obstacle to the comparison with pore size distribution in the never dried CAL-specimens.

## Conclusions

The concretes investigated have zero or very little ice formation before freeze/thaw exposure in the temperature range of the freeze/thaw test, in spite of that they all suffer sever deterioration during the test.

Freeze/thaw deterioration is accompanied by water uptake and increase in amount of freezeable water.

Increased ice formation in the concrete due to freeze/thaw deterioration takes place both in the temperature range of the frost test and in the low temperature region. Some of the increase in evaporable water content after freeze/thaw is not freezeable even down to -55 °C, indicating both strong binding of some of the absorbed water, and changes in the very fine pore structure of the concrete.

The calorimeter results of self healed specimens show that self healing reduced amount of freezeable water both in the temperature range of the frost test and in the low temperature range.

The increased uptake of water and the ice formation measurements show that rather small increase in freezeable water content can lead to large deterioration. The results indicate that this increase is smaller for high strength concretes. It is suggested that the deterioration is progressive, starting from the surface where the water content and the ice formation increases first.

**Acknowledgment**

Thanks to The Norwegian Research Council/Norcon-Lightcon programs, Public Roads Laboratory, Norcem and Norwegian Contractors for financial support, and to Dr. Dirch Bager of Aalborg-Portland for comments and suggestions.

**References**

1. Sellevold, E.J., Jacobsen S., Bakke J.A.: The Int. Worksh. on Freeze/thaw and Deicing Salt Scaling Res. of Conc. Québec, Canada Ed.: J.Marchand and M.Pigeon, pp. 155-165 (1993)
2. Verbeck G., Klieger P.: PCA Research Department Bulletin 95, pp.9 - 22 (1958)
3. Sellevold E.J. and Bager D.H.: 7th Int. Congr. Chem. of cement Vol IV, pp. 394-399 (1980)
4. le Sage de Fontenay, C. and Sellevold E.J.: ASTM STP 691 pp. 425-438 (1980)
5. Bager D.H. and Sellevold E.J.: ASTM STP 691 pp. 439-454 (1980)
6. Bager D.H. and Sellevold E.J.: Cem. and Conc. res. Vol.16, pp.835-844 (1986)
7. Bager D.H.: Technical report 141/84, Techn. Univ. of Denmrk, 66 p. (1984)
8. Hammer T.A., Sellevold E.J.: ACI SP - 121 pp. 457 - 489 (1990)
9. Jacobsen S., Gran H.C., Sellevold E.J., Bakke J.A, acc. for publ. Cem. and conc. res.(1995)
10. Jacobsen S., Marchand J. and Hornain H., acc. for publ. in Cem. and conc. res. (1995)
11. Jacobsen S., Sellevold E.J., paper submitted to Cem. and conc. res (1995)
12. Jacobsen S., Sellevold E.J.:Consec'95, Sapporo, Japan, pp.114-125 Chapmann & Hall (1995)
13. Jacobsen S., Hammer T.A., Sellevold E.J.: Proc. Int. Symp. on Structural LWA concrete, pp.541-554, Norwegian Concrete Association, (1995)
14. Sellevold E.J.: Report O 1731 The Norwegian Building Research Institute, 1986
15. Matala S.: PhD-thesis, Helsinki University of Technology CT-Report 6 (1995)
16. Sellevold E.J., Bager D.H., Klitgaard Jensen E. and Knutsen T.: Report BML 82.610 The Norwegian Institute of Technology pp.19-50 (1982)
17. Fagerlund G.: Report TVBM-3056, Lund Inst. of Techn., Div. of Building Materials (1993)